J Fluoresc (2015) 25:1615–1628
DOI 10.1007/s10895-015-1648-4

ORIGINAL ARTICLE

Novel Iminocoumarin Derivatives: Synthesis, Spectroscopic and Computational Studies

Santosh B. Chemate[1] · **Nagaiyan Sekar**[1]

Received: 1 June 2015 / Accepted: 18 August 2015 / Published online: 11 September 2015

Abstract Three novel iminocoumarin derivatives with high quantum yield are synthesized from 3-benzimidazole substituted coumarin and different aromatic aldehydes. The photophysical behavior of the synthesized compounds was studied using UV-visible and fluorescence spectroscopy in polar and non-polar solvents. The compounds show absorption maxima at around 450 nm and emission maxima at around 500 nm. The quantum yields of compounds in dichloromethane and chloroform are more than 0.90. The absorption, emission and quantum yield of compounds are dependent on the polarity of solvents. Along with an intense absorption, these compounds show shoulder absorption peak in the studied solvents. The solvent polarity plots revealed the charge transfer process in the synthesized molecules from donor to acceptor. Density Functional Theory and Time Dependent Density Functional Theory computations have been used to have more understanding of the structural, molecular, electronic and photophysical parameters of the dyes. The dyes were characterized by FT-IR, ^{1}H NMR, ^{13}C NMR and mass spectral analysis.

Keywords Coumarin · Iminocoumarin · DFT · TD-DFT · Quantum yield

Introduction

In recent years, synthesis and applications of fluorescent materials happen to be a fruitful research activity [1–4]. In the field of functional materials, designing and development of innovative fluorescent molecules for high-tech applications is very demanding [1–4]. The coumarin derivatives have been one of the most widely studied classes of fluorescent dyes, and probably one of the most frequently used fluorescent compounds [5–7]. Fluorescent coumarin derivatives have been widely used in many applications such as fluorescent whitening agents [8], metal sensing [9], cell biology [10, 11], laser dyes [12, 13], pH sensors [14], dye sensitized solar cell (DSSc) [15, 16] and in nonlinear optics [17]. Coumarin itself is non fluorescent but it exhibits intense fluorescence after its substitution by various functional groups at different positions [18]. The fluorescence properties of coumarin can be tuned by incorporating electron donating and accepting groups at different positions on the basic unit. A study of literature reveals that, electron donor substitution at 7-position along with acceptor at 3-position gives red shifted absorption, because such substitution pattern leads to an effective donor acceptor chromophore [1, 19]. The strength of the electron donors and acceptors are also helpful to change the fluorescence properties of the coumarin derivatives. To avoid intersystem crossing and achieve high fluorescence intensity with large Stoke's shift, fused coumarin derivatives are

Electronic supplementary material The online version of this article (doi:10.1007/s10895-015-1648-4) contains supplementary material, which is available to authorized users.

✉ Nagaiyan Sekar
n.sekar@ictmumbai.edu.in

[1] Tinctorial Chemistry Group, Department of Dyestuff Technology, Institute of Chemical Technology, Mumbai 400 019, India

reported in the literature for different applications [20, 21]. Also the dye julolidine-coumarin has 3–5 times greater photochemical stability than that of rhodamine 6G and high energy efficiency compared with the other coumarins [22].

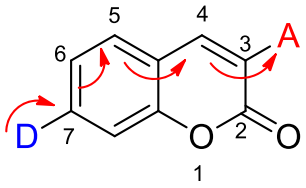

Iminocoumarin is a subclass of coumarin family [23], and very few reports are available in the literature describing the optical properties of iminocoumarins [24–26]. The reported iminocoumarin derivatives bear an electron-releasing group in the 7-position and an electron-acceptor group in the 3-position, a choice probably justified by the fact that this substitution pattern leads to enhanced absorption and fluorescence efficiency in the closely related coumarin series. In the known iminocoumarins, the electron donors are N,N-dialkyl groups at 7 position and electron acceptors like benzothiazole or benzimidazole or cyano group at 3-position which enhance the fluorescence efficiency. The iminocoumarin derived fluorophores are known for their high fluorescence ability and efficient quantum yield and hence are used for metal sensors [9, 26], biological system [27], pH sensor [28] and lasers [24]. The attachment of an ester or amide group in the 3-position leads to a dye with interesting lasing properties and high sensitivity to solvent effects [29]. Most of the iminocoumarin fluorophores emit in the blue green region [19, 30]. As many biological samples also emit in the blue green region of the spectrum, this would interfere with the fluorescence signals generated from the coumarin or iminocoumarin derived fluorophores [25]. This is a limitation of iminocoumarin which emit in the blue-green region. Considering fluorescence properties of iminocoumarin, those which emit beyond 500 nm are demanding in functional applications. This will be achieved by changing donor or acceptors units. The reaction between the aromatic aldehydes with 3-benzimidazol-2-yl-2-iminocoumarin leads to a rigid molecular structure. In the present paper, instead of playing with donor and acceptor units we have synthesized rigid iminocoumarin from 3-benzimidazol-2-yl-2-iminocoumarin and aromatic aldehydes (Schemes 1 and 2). The two different aromatic aldehydes were used bearing different spacer groups. The length of spacer groups plays important role during the binding of fluorescent probes with the biomolecules. The purpose of fused iminocoumarin designing was to achieve the planarity which will enhance electron flow within the conjugated ring system and to avoid intersystem crossing due to free rotation of groups present at 3-position on coumarin unit [25, 31].

Result and Discussion

Chemistry

Three novel iminocoumarin derivatives **5a-b** and **12** have been synthesized from iminocoumarin **3** or **11** and aromatic aldehydes **4a-b** or **10**. The aromatic aldehydes **4a-b** were obtained by Vilsmeier Haack formylation reaction of corresponding aromatic amines [32]. 2-cyanomethyl benzimidazole **1** was prepared from *o*-phenylene diamine and ethylcyanoacetate in o-xylene [33]. The iminocoumarin **3** and **11** was prepared from 2-cyano methyl benzimidazole **1** and *o*-hydroxy aldehyde **2** or **10** by a condensation followed by cyclization reaction in the presence of catalytic amount of piperidine. The structures of the dyes were confirmed by FT-IR, ^{1}H NMR, ^{13}C NMR and mass spectral analysis. The absorption and emission spectra were measured to investigate the photophysical properties and also the solvatochromism and solvatofluorism behaviors of the molecule were studied by measuring the absorption and emission spectra in the solvents.

Photophysical Properties

The UV-Vis absorption and fluorescence emission of the fused iminocoumarin **5a**, **5b** and **12** in solvents of varying polarities are reported in Table 1**,** and absorption and emission spectra are shown in Figs. 1, 2 and 3. The compounds **5a**, **5b** and **12** are fluorescent in solution. The absorption and emission properties of the compounds **5a**, **5b** and **12** were evaluated in different solvents and the results revealed that the compounds **5a**, **5b** and **12** are sensitive towards the solvent polarities. The compound **5a** shows short wavelength and long wavelength absorption in the visible region. The short wavelength absorption is intense between 425 to 443 nm and long wavelength absorption (shoulder peak) is between 447 to 467 nm. Similarly, the compound **5b** showed short wavelength absorption maxima between 430 to 443 nm and longer wavelength absorption maxima between 455 to 468 nm. The two absorption peaks observed, may be due to the cross conjugation present in the molecule **5a** and **5b**. The absorption and emission properties for **5a** and **5b** are almost similar. The spacer (R group) present on nitrogen atom does not have any influence on spectroscopic properties. The compound **12** also shows dual absorption in chloroform, ethylacetate and 1,4 dioxane solvents. The shorter wavelength maxima is at 452 nm in chloroform, 430 nm in ethyl acetate and 443 nm in 1,4 dioxane and long wavelength absorption is at 471 nm in chloroform, 453 nm in ethylacetate and 462 nm in 1,4 dioxane. The compound **12** shows red shifted absorption and emission as compared to the compounds **5a** and **5b**.

Scheme 1 Synthesis of iminocoumarin derivative 5a-b

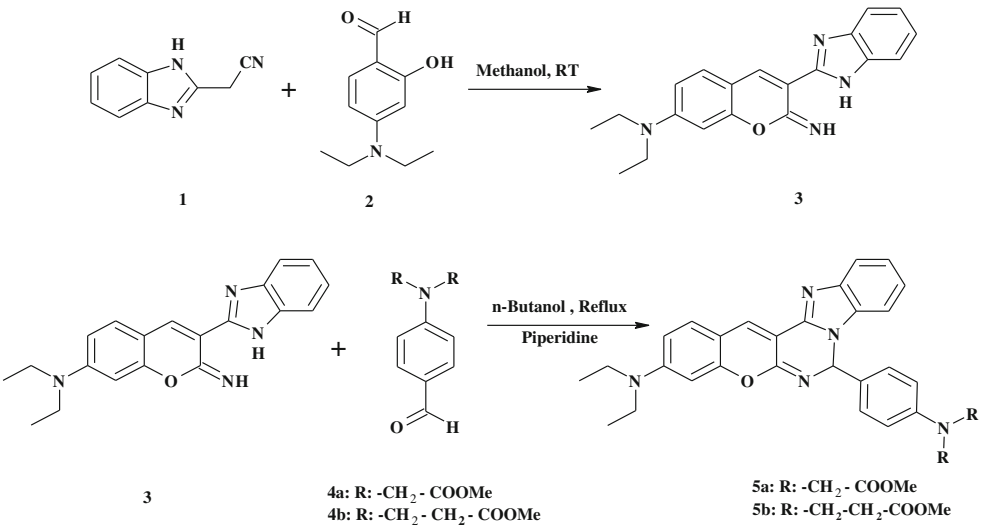

The red shifted absorption as well as emission of compound **12** are due to the strength and rigidity of the electron donor unit. Due to planarity, the molecule **12** could undergo aggregation which can be responsible for changes in shape and intensity of absorption and emission spectra. The iminocoumarin derivatives have more solubility in polar solvents than the less polar solvents. The compound **5a** shows intense absorption in acetone, acetonitrile, methanol, ethanol and chloroform. In the case of compound **5b**, the absorption pattern is almost similar in all the studied solvents except 1,4 dioxane. The fluorescence properties of the compounds in different solvents were measured to study solvofluorism property. The excitation wavelength used for the fluorescence measurements was absorption maxima of the compounds in respective solvents. The fluorescence emission of the compounds are sensitive towards the solvent properties Table 1. The compounds show positive solvotoflurosium. These coumarins showed a blue-shifted fluorescence emission maxima in non-polar solvents and red-shifted fluorescence emission maxima in the polar solvent. The compound **5a** shows a red shifted emission in the polar solvents (methanol, ethanol, DMSO and acetonitrile) and the blue shifted emission in the less polar solvents (acetone, DCM, chloroform,

Scheme 2 Synthesis of iminocoumarin 12

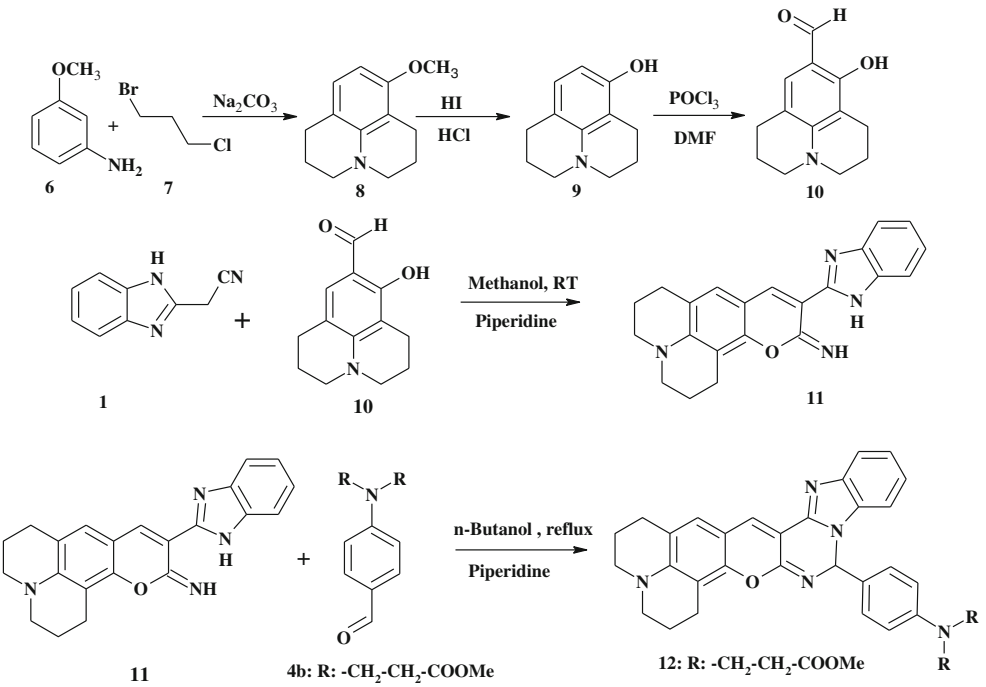

Table 1 The UV-Vis absorption and fluorescence emission of compounds **5a**, **5b** and **12** in solvents of varying polarities

Dye	Solvents	λ_{abs}nm	λ_{ems}nm	Stokes shift (cm^{-1})	Є ($mol^{-1}cm^{-1}$)	*f*	ϕ_f
5a	MeOH	443[a] 467[b]	502[a]	2653[aa] 1493[ab]	21,000	0.8252	0.67
	EtOH	442[a] 467[b]	502[a]	2653[aa] 1493[ab]	23,000	0.8120	0.61
	DMSO	440[a] 462[b]	502[a]	2807[aa] 1725[ab]	21,000	0.6622	0.48
	Acetone	434[a] 458[b]	492[a]	2716[aa] 1509[ab]	23,000	0.9764	0.45
	DCM	437[a] 461[b]	488[a] 518[b]	2391[aa] 2387[bb]	23,000	0.7936	0.93
	$CHCl_3$	440[a] 464[b]	490[a] 514[b]	2319[aa] 2096[bb]	20,000	0.7241	0.94
	EA	425[a] 447[b]	481[a] 506[b]	2739[aa] 5649[bb]	20,000	0.7856	0.70
	ACN	435[a] 455[b]	494[a]	4707[aa] 3696[ab]	21,000	0.8255	0.77
	1,4 Dioxane	430[a] 453[b]	478[a] 508[b]	2335[aa] 2273[ab]	22,000	0.1949	0.27
	DMF	438[a] 460[b]	497[a]	2710[aa] 1618[ab]	19,000	0.6753	0.82
5b	MeOH	443[a] 468[b]	500[a]	2573[aa] 1368[ab]	33,000	2.8230	0.63
	EtOH	443[a] 467[b]	502[a]	4258[aa] 3098[ab]	37,000	3.4292	0.53
	DMSO	443a 462 [b]	506[a]	4811[aa] 3883[ab]	33,500	1.4445	0.39
	Acetone	434[a] 455 [b]	491[a]	2675[aa] 1611[ab]	37,000	3.2304	0.49
	DCM	438[a] 463[b]	490[a] 518[b]	3783[aa] 2551[bb]	40,000	0.7716	0.92
	$CHCl_3$	440[a] 463[b]	499[a] 516[b]	2151[aa] 2143[bb]	380,000	3.1265	0.94
	EA	443[a] 465[b]	481[a]	1783[aa] 715[ab]	37,000	1.1626	0.73
	ACN	437[a] 456 [b]	494[a]	2640[aa] 1687[ab]	38,000	3.9317	0.81
	1,4 Dioxane	430[a] 455 [b]	476[a] 510 [b]	2247[aa] 2370[bb]	29,000	4.1789	0.43
	DMF	438[a] 456[b]	495[a]	2629[aa] 1728[ab]	38,000	2.0235	0.82
12	MeOH	464	505	1982	56,660	0.8531	0.62
	EtOH	464	510	3270	51,890	0.8298	0.52
	DMSO	464	512	3631	20,810	0.3002	0.61
	Acetone	464	501	1592	70,600	1.5819	0.62
	DCM	470	498	2758	39,400	0.6351	0.94
	$CHCl_3$	452[a] 471[b]	496[a]	2044[aa] 1151[ab]	35,760	0.5446	0.95
	EA	430[a] 453[b]	498[a]	3175[aa] 1995[ab]	17,660	0.2456	0.56
	ACN	465	510	1898	75,680	1.1908	0.89
	1,4 Dioxane	443[a] 462[b]	491[a]	2207[aa] 1278[ab]	16,600	0.2734	0.42
	DMF	464	512	2020	22,200	0.6531	0.77

[a] Intense peak, [b] Shoulder peak, [aa] Stokes shift for intense absorption wavelength and emission wavelength, [ab] Stokes shift between shoulder peak absorption wavelength and emission wavelength, [bb] Stokes shift between shoulder peak absorption wavelength and longer emission wavelength, ε = molar extinction coefficient, *f* = Oscillator Strength

MeOH: Methanol, EtOH: Ethanol, EA: Ethyl acetate, DMSO: Dimethylsulfoxide, DCM: Dichloromethane, $CHCl_3$: Chloroform, DMF: n, n dimethyl formamide, ACN: Acetonitrile

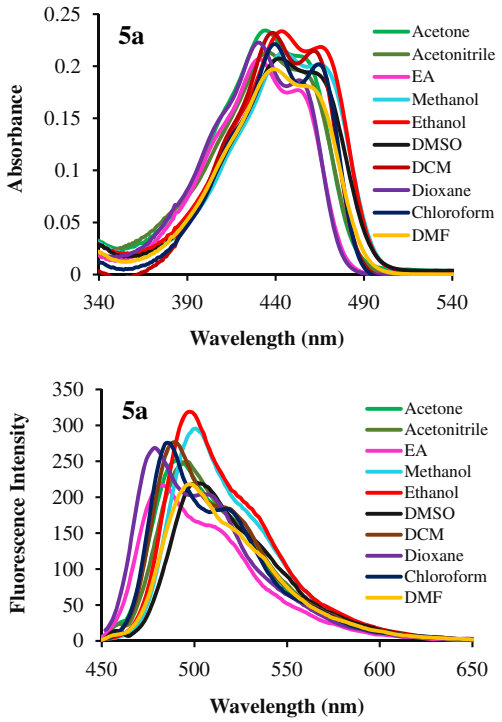

Fig. 1 Absorption and emission spectra of compound **5a** in different solvents

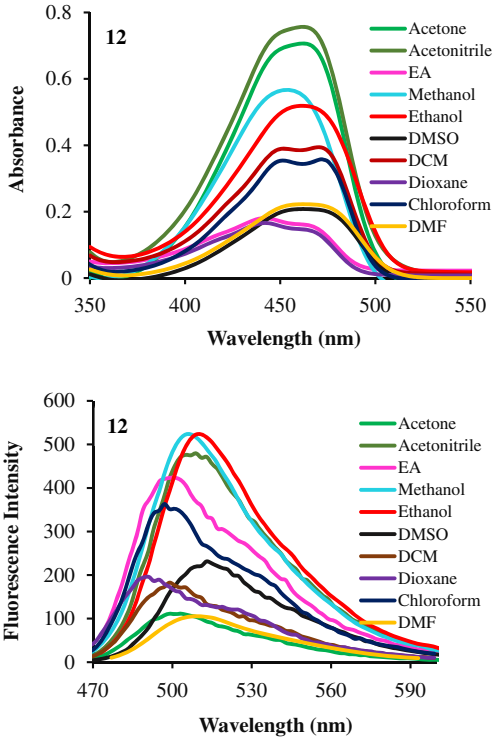

Fig. 3 Absorption and emission spectra of compound **12** in different solvents

ethylacetate and dioxane). Along with the intense emission, the shoulder peak is observed for the compound **5a** in the studied solvents. The intense peak is due to the short wavelength emission and the shoulder peak due to the long wavelength emission. The compound **5a** shows emission band at around 500 nm in polar solvents and around 490 nm in nonpolar solvents. Similar emission pattern is observed for the compound **5b**. The compound **5b** shows red shifted emission in methanol, and DMSO at around 500 nm and blue shifted intense emission in methanol, acetone, DCM, chloroform, ethylacetate, dioxane and acetonitrile at around 490 nm with the shoulder peak at around 510 nm. The fluorescence quantum yield of the compound **5b** is less in 1,4 dioxane as compared to other solvents. The compound **12** shows a red shifted emission as compared to the compounds **5a** and **5b.** The emission spectra of the compound **12** in different solvents are also broad as compared to the compound **5a** and **5b**. A red shifted emission was observed at around 510 nm for the compound **12** in DMSO, ethanol, acetonitrile and DMF and a blue shifted emission at around 500 nm in acetone, methanol, ethylacetate, DCM, chloroform was observed. The molar extinction coefficient of the dyes varied from 19,000 to 75,680 mol^{-1} cm^{-1}. The dye **5b** have higher molar extinction coefficient values than the dye **5a**. However, the dye **12** shows higher molar extinction coefficient values than the dye **5a** and **5b**.

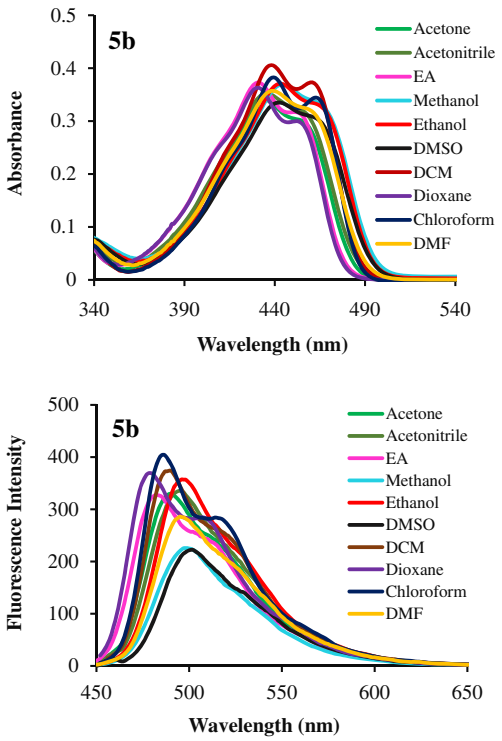

Fig. 2 Absorption and emission spectra of compound **5b** in different solvents

The fluorescence quantum yields of the synthesized coumarins were determined in different solvents and tabulated in Table 1. The fluorescence quantum yields of the coumarins largely depend on the solvent polarity shown in Table 1. The

three coumarins showed quantum efficiencies >0.90 in dichloromethane, chloroform and the lowest quantum yield in 1, 4 dioxane. The quantum yield of the compound **5a** is very high in chlorinated solvents like dichloromethane, chloroform (>0.90) while in other solvents such as DMF, ethyl acetate, acetonitrile and methanol it is more than 0.6. The compound **5a** shows low quantum yield in 1, 4-dioxane (0.27). A similar trend is observed for compound **5b**. The quantum yields of the compound **12** in the solvents such as dichloromethane, chloroform, acetonitrile, and 1,4 dioxane are high as compared to the compounds **5a** and **5b**. In compound **12** rigid fixing of the diethylamino group by two saturated six-membered heterocycles leads to red shift in absorption and emission. From photophysical study it is observed that rigid fixing of electron donor group in iminocoumarin dyes not only shift absorption and emission towards longer wavelength but also increases the fluorescence intensity.

Solvent Polarity Plots and Intramolecular Charge Transfer

The Stokes shift increases with increase in the solvent polarity which indicates an extensive structural re-organization in the excited state [34]. This shows that these coumarins have polar excited state and it is more stabilized in the polar solvent. This confirms the intramolecular charge transfer characteristics of these coumarins [34]. The solvatochromic behaviour of the molecules was studied with the help of Lippert plot [35] and Weller Plot [36]. Lippert's plot is the plot of stokes shift in cm^{-1} vs orientation polarizability. The Lippert function is constituted of the polarity function $f(\varepsilon)$ and polarizability function $f(\eta)$ shows good correlation which supports the intramolecular charge transfer in the synthesized dyes (Figure S1, Table S1). The Weller plots shows good linear behaviour which is indicative of charge transfer at excited state in these molecules. Thus the emission is highly sensitive towards the polarity of the solvents (Figure S2). All the dyes responds well to the solvent polarity functions (ε, n), the similar equations are introduced by Bilot-Kawski [37] for the estimation of ratio of excited state dipole moment and ground state dipole moment i.e. μ_e/μ_g. The dipole moments calculated with the above equations is given in Table S2. The compounds **5a** and **5b** has μ_e/μ_g ratio higher than compound **12** which suggest that the excited state is more polar than the ground state for these molecules.

Oscillator Strength and Transition Dipole Moment of the Dyes

Oscillator strength is dimensionless quantity that expresses the probability of absorption and emission properties in energy levels, which helps to understand charge transfer within the molecules. It was simply described number of electron transition from ground to excited state. Oscillator strength (f) can be calculated using the following Eq. 1 [38]. Where ε is the extinction coefficient (L mol^{-1} cm^{-1}), and ν represents the wavenumber (cm^{-1}). From this equation we have calculated oscillator strength for iminocoumarin derivatives and tabulated in Table S3.

$$f = 4.32 \times 10^{-9} \int \varepsilon(\nu) d\nu \tag{1}$$

By using the value of f, we have calculated transition dipole moment that was the differences in electric charge distribution between a ground and excited state of the molecule. The transition dipole moment for absorption (μ_{ge}) is a measure of the probability of radiative transitions which have been calculated form of Debye in different solvent environments using the Eq. 2 [38]. The transition dipole moment was increased with increase in the oscillator strength.

$$\mu_{ge}^2 = \frac{f}{2.13 \times 10^{-30} \times \nu} \tag{2}$$

Where,
μ_{ge} is transition dipole moment (D),
f is oscillator strength,
ν is wavenumber (cm^{-1}).

The molar extinction co-efficient (ε) and apparently the transition dipole moments (μ_a) are higher for **12** than compound **5a** and **5b** (Table S3). This clearly indicates effective charge transfer in compound **12** due to rigidity at donor part.

DFT and TD-DFT Computations

All the computations were performed with the Gaussian 09 package [39]. DFT method was used for the ground state optimization, while for the excited state optimization, time-dependent density functional theory (TD-DFT) was used. The hybrid functionals namely B3LYP (Becke3-Lee-Yang-Parr hybrid functional) [40–43] was used. The 6-31G(d) basis set was used for all atoms and later was ascertained in the literature [44]. The Polarizable Continuum Model (PCM) [45] was used to optimize the ground and excited state geometries. The excitation energies, oscillator strengths and orbital contribution for the lowest 10 singlet-singlet transitions at the optimized geometry in the ground state were obtained by TD-DFT calculations using the same basis set as for the geometry minimization. The solvents used were methanol (MeOH), acetonitrile (ACN), *N*,*N*-dimethyl formamide (DMF), dimethylsulfoxide (DMSO), ethanol (EtOH), 1,4 dioxane, ethyl acetate (EA), chloroform ($CHCl_3$), dichloromethane (DCM) and acetone.

To gain more insight into the electronic properties of the compounds, density functional theoretical (DFT) and Time-dependent density functional theory (TD-DFT) calculations were performed for the compounds **5a, 5b** and **12** with the Gaussian 09 program package. The structures of compounds **5a-b** and **12** were optimized using the B3LYP functional and 6- 31G(d) basis set. The theoretical predictions about the vertical excitation, oscillator strength and their orbital contributions are summarised in Tables 2, 3 and 4. The experimental absorption and vertical excitation data are in good agreement for compound **5b** as compared to compounds **5a** and **12**. The compound **5a** shows dual absorption, short wavelength absorption around 438 nm and long wavelength absorption was around 460 nm. The short wavelength absorption in studied solvents is in good agreements with vertical excitation. For compound **5a** the lower deviation in experimental absorption and vertical excitation was observed in ethyl acetate 3 nm, while for methanol 20 nm deviation is observed. This vertical excitation is due to HOMO to LUMO transition. In ethanol and methanol **5a** shows large deviation between long wavelength absorption and vertical excitation (44 nm). This vertical excitation is due to HOMO to LUMO transition (98 %) with high oscillator strength (1.23). In other solvents **5a** shows 10 to 15 nm deviation between short wavelength absorption and vertical excitation (Table 2). Compound **5b** also shows dual absorption, short wavelength absorption and long wavelength absorption about 437 and 460 nm respectively. The short wavelength absorption in studied solvents is in good agreements with vertical excitation. The compound **5b** shows the lower deviation in experimental short wavelength absorption and vertical excitation in acetone (9 nm), DMF (11 nm), acetonitrile (12 nm) and 1,4 dioxane (8 nm) (Table 3). In the case compound **12** the deviation between experimental absorption and vertical excitation is more in methanol, acetonitrile, DMF, DMSO, ethanol, acetone, DCM and chloroform (~30 nm). Compound **12** shows 2 nm deviation in absorption and vertical excitation in ethyl acetate (Table 4).

The experimental fluorescence emissions were compared with TD-DFT emission for compounds **5a-b** and **12**. The compounds **5a** and **5b** shows duel emission in less polar solvents. For compound **5a**, deviation between experimental emission and TD-DFT emission was very less for shorter emission while higher deviation was observed for longer experimental emission and TD-DFT emission. The compound **5a** shows lower deviation in shorter emission and TD-DFT emission in 1,4 dioxane (8 nm) and ethyl acetate (13 nm) and

Table 2 Experimental and computed absorption and emission of the dye **5a** in different solvents

Solvent	Experimental		TD-DFT						
	λabs[a] (nm)	λems[b] (nm)	Vertical Excitation[c] (nm)	ev	*f*[d]	Assignment	% D[e] (abs)	TD-DFT Emission	% D[f] (ems)
MeOH	443 467	502	423	2.9343	1.2210	H-L = 98 %	4.5 9.4	467	7.0
EtOH	442 467	502	423	2.9293	1.2316	H-L = 98 %	4.3 9.4	468	6.8
DMSO	440 462	502	425	2.9169	1.2511	H-L = 98 %	3.4 8.0	471	6.2
Acetone	434 458	492	423	2.9308	1.2302	H-L = 98 %	2.5 7.6	468	4.9
DCM	437 461	488 518	424	2.9268	1.2476	H-L = 98 %	3.0 8.0	470	3.7 9.3
$CHCl_3$	440 464	490 514	423	2.9341	1.2492	H-L = 98 %	3.9 8.8	471	3.9 8.4
EA	425 447	481 506	422	2.9420	1.2282	H-L = 98 %	0.7 5.6	468	2.7 7.5
ACN	435 455	494	423	2.9309	1.2267	H-L = 98 %	2.8 7.0	469	5.1
1,4 Dioxane	430 453	478 508	419	2.9581	1.2295	H-L = 98 %	2.6 7.5	470	1.7 7.5
DMF	438 460	497	425	2.9153	1.2548	H-L = 98 %	3.0 7.6	471	5.2

[a] Experimental absorption wavelength

[b] Experimental emission wavelength

[c] Computed absorption wavelength

[d] Oscillator strength

[e] % Deviation between experimental absorption and vertical excitation computed by DFT

[f] % Deviation between experimental emission and computed (TD-DFT) emission

Table 3 Experimental and computed absorption and emission of the dye **5b** in different solvents

Solvent	Experimental		TD-DFT						
	λabs[a] (nm)	λems[b] (nm)	Vertical Excitation[c] (nm)	ev	f^d	Assignment	% D[e] (abs)	TD-DFT Emission	% D[f] (ems)
MeOH	443	500	424	2.9229	1.1194	H-L = 98 %	4.3	471	5.8
EtOH	443	502	425	2.9184	1.1332	H-L = 98 %	4.1	472	6.2
DMSO	443	506	425	2.9218	1.1301	H-L = 98 %	4.1	473	6.5
Acetone	434	491	425	2.9199	1.1307	H-L = 98 %	2.1	472	3.9
DCM	438	490 518	425	2.9167	1.1509	H-L = 98 %	3.1	475	3.1 8.3
$CHCl_3$	440	499 516	425	2.9165	1.0738	H-L = 98 %	3.5	507	1.6 1.7
EA	443	481	424	2.9229	1.0385	H-L = 98 %	4.5	475	1.2
ACN	437	494	425	2.9198	1.1276	H-L = 98 %	2.8	472	4.5
1,4 Dioxane	430	476 510	422	2.9402	1.0529	H-L = 98 %	1.9	526	9.5 3.0
DMF	438	495	427	2.9053	1.1656	H-L = 98 %	2.5	475	4.0

[a] Experimental absorption wavelength

[b] Experimental emission wavelength

[c] Computed absorption wavelength

[d] Oscillator strength

[e] % Deviation between experimental absorption and vertical excitation computed by DFT

[f] % Deviation between experimental emission and computed (TD-DFT) emission

38 nm deviation was observed longer emission (Table 2). The shorter wavelength emission deviation for other solvents was slightly higher (such as for methanol 35 nm, Ethanol 34 nm, DMSO 31 nm, Acetone 24 nm, DCM 18 nm, $CHCl_3$ 19 nm, Acetonitrile 25 nm, DMF 26 nm) while emission deviation in longer wavelength was higher for DCM 48 nm. The deviation

Table 4 Experimental and computed absorption and emission of the dye **12** in different solvents

Solvent	Experimental		TD-DFT						
	λabs[a] (nm)	λems[b] (nm)	Vertical Excitation[c] (nm)	ev	f^d	Assignment	% D[e]	TD-DFT Emission	% D[f] (ems)
MeOH	464	505	435	2.8536	1.1137	H-L = 98 %	6.3	476	5.7
EtOH	464	510	435	2.8494	1.1267	H-L = 98 %	6.3	477	6.5
DMSO	464	512	437	2.8362	1.1506	H-L = 98 %	5.8	479	6.4
Acetone	464	501	435	2.8514	1.1250	H-L = 98 %	6.3	477	4.8
DCM	470	498	435	2.8512	1.1463	H-L = 98 %	7.4	479	3.8
$CHCl_3$	452	496	433	2.8628	1.1483	H-L = 98 %	4.2	480	3.2
EA	430	498	432	2.8684	1.1222	H-L = 98 %	0.5	477	4.2
ACN	465	510	435	2.8502	1.1207	H-L = 98 %	6.5	477	6.5
Dioxane	443	491	428	2.8938	1.1328	H-L = 98 %	3.4	481	2.0
DMF	464	512	436	2.8429	1.2214	H-L = 98 %	6.0	480	6.3

[a] Experimental absorption wavelength

[b] Experimental emission wavelength

[c] Computed absorption wavelength

[d] Oscillator strength

[e] % Deviation between experimental absorption and vertical excitation computed by DFT

[f] % Deviation between experimental emission and computed (TD-DFT) emission

between shorter wavelength emission and TD-DFT emission was less than longer wavelength emission (Table 4). For compound **12** the deviation in emission was observed more in polar solvents around 33 nm while in less polar solvents emission deviation was around 12 nm (Table 4).

The dihedral angles optimized at the ground state (GS) and excited state (ES) suggests that planarity increases in the excited state (Table S4). The dihedral angle between 7-N, N diethyl amino group and phenyl ring of coumarin in the optimised structure of **5a** is 179.9 (GS) and dihedral angle between coumarin unit and benzimidazole group is 178.9 (GS) indicates the structure is coplanar (Fig. 4). Based on these geometrical optimizations, we found that the coumarin unit is almost coplanar with the benzimidazole, leading to effective π-conjugation throughout the molecules (Fig. 4). The dihedral angle between iminocoumarin unit and n-substituted benzene (receptor) is −125.2 (GS) which indicates the iminocoumarin unit and n-substituted benzene is nonplanar. The n-substituted benzene part is attached to tetrahedral carbon and expected dihedral angle in 109. Similar observation is observed for **5b** (Fig. S4). For compound **12** is the dihedral angle between 7-position electron donor nitrogen atom and phenyl ring of coumarin in the optimised structure is 172.7 (GS) (Fig. S4). The contribution of electronic transition from HOMO to LUMO is about 98 % in **5a**, **5b** and **12**. Therefore, we confirm that electronic transitions of both compounds are originated from HOMO to LUMO. As shown in Table 5, all the compounds show that electron transfer from the donor to the acceptor segment occurs effectively. The HOMO levels of **5a**, **5b** and **12** are mainly dominated by π-orbital contribution of the N, N diethyl electron donor unit, while the LUMO levels are largely delocalized at the electron acceptor unit of benzimidazole (Table 5). Also from bond length and bond angle data of **5a**, **5b** and **12** clearly suggested that the charge transfer from electron donor to acceptor unit (Table S4**).** This indicates that the charge separation increases in the excited state which results in a larger dipole moment than that in the ground state. It also explains the sensitivity of the fluorescence emission spectra of these push-pull dipolar dyes to the solvent polarities.

Experimental

Methods and Materials

All the commercial reagents and solvents were purchased from S. D. Fine Chemicals Pvt. Ltd. and used without purification and all the solvents were of spectroscopic grade. The absorption spectra of the dyes were recorded on a Perkin-Elmer spectrophotometer, Lambda 25, and emission spectra were recorded on Varian Cary Eclipse fluorescence spectrophotometer using freshly prepared solutions in solvents of different polarities at a concentration of 1×10^{-6} mol L^{-1}. The photophysical properties were investigated using the solvatochromic and solvatofluoric behaviors of the dyes. The excitation wavelength used for the fluorescence measurements was absorption maxima of the compounds in respective solvents. The FT-IR spectra were recorded on a Jasco 4100 Fourier Transform IR instrument (ATR accessories). ^{1}H NMR and ^{13}C NMR spectra were recorded on Varian 500 MHz instrument using TMS as an internal standard. Mass spectra were recorded on Finnigan mass spectrometer.

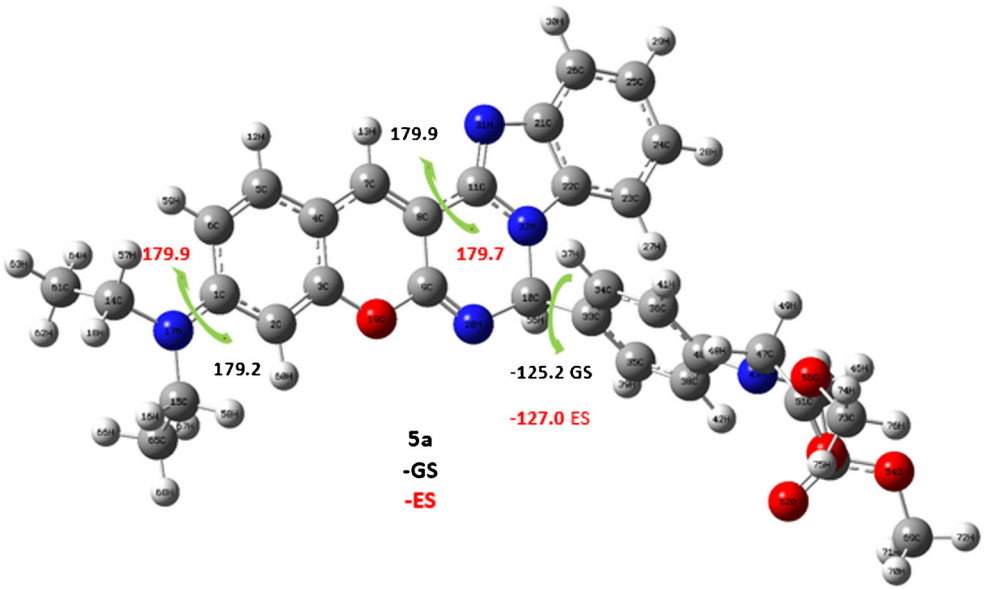

Fig. 4 Optimized geometry parameters of dye **5a** in methanol solvent in the ground state and excited state (dihedral angles are in degree)

Table 5. FMO diagrams for compound **5a-b** and **12** calculated with B3LYP/6-31G(d) method in methanol

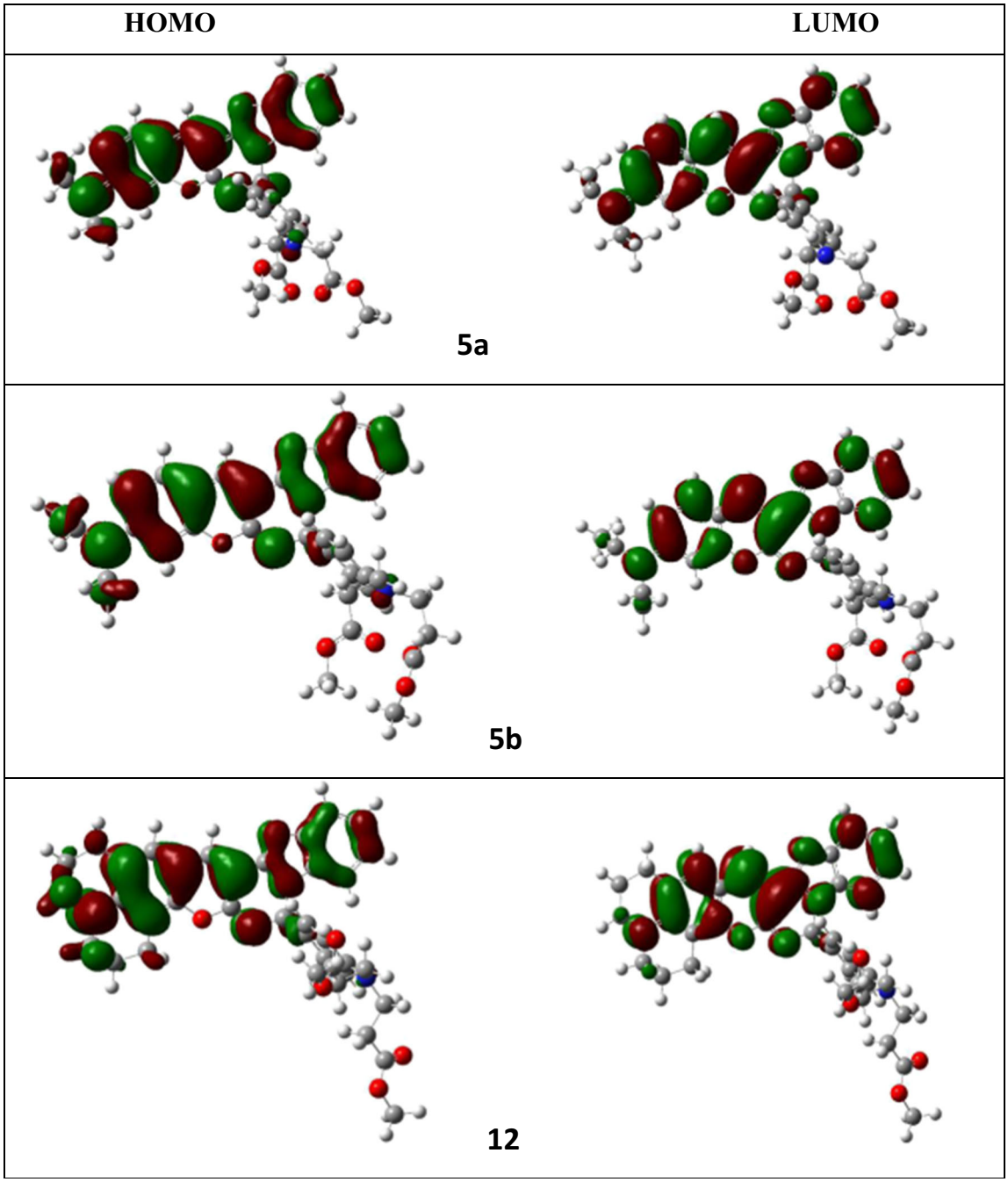

Relative Quantum Yield Calculations

The quantum yields of the compounds **5a-b** and **12** in different solvents were evaluated. Fluorescence quantum yields were evaluated with respect to 3-(2-benzothiazolyl)-7-diethylaminocoumarin (Coumarin-6) in ethyl alcohol (ϕ = 0.78) [46]. The quantum yield values were calculated using the comparative method [47–49]. The absorption and emission characteristics of the standards and for the compounds in polar as well as non-polar solvents were measured at different concentrations at room temperature. The fluorescence measurements were performed with solution containing molecular oxygen. The emission intensity values were plotted against the absorbance values and linear plots were obtained. The gradients were calculated for the compounds in each solvent and for the standards. All the measurements were done

by keeping the parameters such as solvent and slit width constant. The relative quantum yields of the synthesized compounds in different solvents were calculated using the Eq. 3 [47–49].

$$\phi_x = \Phi_{st} \times \frac{Grad_x}{Grad_{st}} \times \frac{{\eta_x}^2}{{\eta_{st}}^2} \quad (3)$$

Where:

Φ_x	Quantum yield of compound
Φ_{st}	Quantum yield of standard sample
$Grad_x$	Gradient of compound
$Grad_{st}$	Gradient of standard sample
η_x	Refractive index of solvent used for synthesized compound
η_{st}	Refractive index of solvent used for standard sample

Experimental Procedure

Synthesis of Intermediate 1

A mixture of o-phenylene diamine (16.2 g, 0.15 mol) and ethyl cyanoacetate (25.4 g, 0.22 mol) and o-xylene (160 ml) was refluxed for 10–12 h in flask equipped with dean-stark trap. Then the reaction mixture was allowed to stand overnight at room temperature. The obtained solid was filtered and dried. The compound was recrystalised by 95 % ethyl alcohol. Yield =60 %, m.p. 206 °C (lit. 207 °C) [33].

Synthesis of 4-(N,N-diethyl amino)-2-hydroxybenzaldehyde 2

Phosphorous oxychloride ($POCl_3$) (2.75 ml, 0.03 mol) was slowly added to N, N dimethyl formamide (DMF) (3.65 mL, 0.05 mol) at 5–10 °C under constant stirring. To this cooled reagent 3-(*N*,*N*-diethyl amino) phenol (0.01 mmol) in DMF (6 mL) was added slowly under constant stirring and the resulting mixture was heated at 75 °C for 4 h. The reaction mixture was cooled to room temperature and then poured into ice cold water (60 mL). The reaction mass was neutralized with sodium carbonate, brown colored solid separated out. The solid product was filtered and washed with cold water, dried and crystallised from ethanol to obtain the pure product **2**, Yield =80 %, m.p. 62 °C (lit. 62 °C) [50].

Synthesis of 3-Benzimidazole Iminocoumarin 3

To a solution of 2-cyano methyl benzimidazole **1** (0.55 g, 2.8 mmol), piperidine (0.1 mL, 1.4 mmol) was added in dry methanol (50 mL), and the solution was stirred at room temperature for 30 min. Then 4-(*N*, *N*-diethyl amino)-2-hydroxybenzaldehyde (0.49 g, 2.8 mmol) was added. The mixture was stirred for 5 h at room temperature, and the precipitate was collected by filtration, washed with dry methanol, and dried under high vacuum to obtain a yellow solid of 3-benzimidazole iminocoumarin **3**. Yield = 82 %, m.p.238 °C (lit.239 °C) [28].

Synthesis of Coumarin 5a and 5b

A mixture of the iminocoumarin **3** (0.332 g 3 mmol) and the aromatic aldehyde **4a-b** (3 mmol), piperidine (0.1 mL) in *n*-butanol (15 ml) was heated to reflux for 4 h, cooled, and left overnight. The precipitated solid was filtered off, washed with ethanol, and dried. The yellow colored solid **5a-b** obtained was purified by column chromatography.

5a: Yield = 78 %, Orange red solid, **^{1}H NMR** ($CDCl_3$, 500 MHz) δ ppm : 1.18 (t, 6H), 3.37 (s, 6H), 3.71 (s, 4H), 4.34 (m, 4H), 6.34(d, *J* = 2.5 Hz, 1H), 6.4 (dd, *J* = 2.5 Hz & 9 Hz, 1H), 6.54 (d, *J* = 9 Hz, 2H), 7.04 (d, *J* = 9 Hz, 2H), 7.10 (d, *J* = 8 Hz, 1H), 7.20(dd, *J* = 1.5 Hz & 5 Hz, 1H), 7.21(dd, *J* = 1.5 Hz & 5 Hz, 1H), 7.23 (d, *J* = 6 Hz, 1H), 7.26 (s,1H), 7.74 (d, *J* = 8 Hz, 1H), 8.07 (s, 1 H), **^{13}C NMR** ($CDCl_3$, 125 MHz) δ ppm: 12.5, 30.5, 44.9, 65.0, 73.6, 97.8, 105.3, 108.0, 108.4, 111.2, 112.7, 118.9, 122.6, 122.9, 127.2, 129.6, 129.7, 130.0, 133.0, 144.3, 145.4, 148.0, 151.1, 154.1, 155.6, 171.1, FT-IR (cm^{-1}) : 2966 (−C-H, aromatic), 1731 (carbonyl), 1677, 1606 (−C=C-, aromatic), 1551, 1521 (−C=C-), **Mass**: m/z 581.7 $[M + 2]^+$.

5b: Yield = 71 %, Orange red solid, **^{1}H NMR** ($CDCl_3$, 500 MHz) δ ppm: 1.22 (t, 6H), 2.56(t, 4H), 3.42 (m, 4H), 3.64 (t, 4H), 3.67 (s, 6H), 6.42 (d, *J* = 2 Hz, 1H), 6.50 (dd, *J* = 2 Hz & 7.5 Hz, 1H), 6.64 (d, *J* = 7.5 Hz, 2H), 7.03 (d, *J* = 6.5 Hz, 1H), 7.08–7.15 (m, 4H), 7.27 (dd, *J* = 7 Hz & 7.5 Hz, 2H), 7.77 (d, *J* = 7 Hz, 1H), 8.11 (s, 1H), **^{13}C NMR** (125.6 MHz, DMSO-*d6*, ppm, Me_4Si): 12.4, 32.1, 44.8, 46.8, 51.7, 73.6, 97.7, 106.3, 107.9, 108.3, 111.1, 112.5, 118.9, 122.5, 122.8, 127.3, 128.1, 129.6, 129.9, 133.0, 144.4, 145.4, 146.7, 151.0, 154.1, 155.6, 172.4, **FT-IR**(cm^{-1}): 2966 (−C-H, aromatic), 1738 (carbonyl), 1692, 1666 (−C=C-, aromatic), 1572, 1549 (−C=C-), **Mass**: m/z 608.6 $[M + 1]^+$.

Synthesis of 8-methoxy julolidine 8

3-Methoxyaniline **6** (12.3 g, 0.10 mol), 1-bromo-3-chloropropane **7** (235 g,1.5 mol), and anhydrous sodium carbonate (42.7 g, 0.4 mol) were combined in a 500 mL three necked round bottomed flask equipped with an overhead mechanical stirrer, thermometer, and a pressure equalizing addition funnel. The top of the addition funnel was fitted with a condenser. The mixture was heated to 70 °C for 1 h and 100^{O}C for 2 h and then reflux for 11 h. The progress of the

reaction was monitored by TLC. After the completion of reaction, the mixture was cooled to room temperature and 150 mL of concentrated HC1 and 50 mL of water were slowly added. Upon dissolution of all solids, the phases were separated and the organic layer was washed with 10 % HCl to remove remaining product. This washing was added to the aqueous phase, which was washed with ether to remove 1-bromo-3-chloropropane. The aqueous phase was basified with 50 % aqueous sodium hydroxide and extracted with ethyl acetate until the organic phase was no longer colored. The ethyl acetate solution was dried over sodium sulphate, and the solvent was removed under reduced pressure. The resulting brown oil was purified by column chromatography to get pure product. Yield = 64 %, Viscous yellow oil which turned red on exposure to air [20].

8-Hydroxyjulolidine 9

8-Methoxyjulolidine **8** (10 g, 50 mmol) was dissolved in a solution consisting of 50 mL of 47 % HI, 80 mL of concentrated HC1, and 200 mL of water. The reaction mixture was refluxed and the progress of the reaction was monitored by TLC. After 15 h another 50 mL concentrated HCl was added to the reaction. The reaction completed within 60 h. The solution was cooled in an ice bath and neutralized to pH 6 first using 50 % NaOH and then phosphate buffer was added (6.9 g of $NaH_2PO_4.H_2O$ and 1.4 g of Na_2HPO_4 in 100 mL of H_2O). The product was extracted with dichloromethane, the organic phase was washed with brine and dried over Na_2SO_4, and the solvent was removed under reduced pressure. The obtained crude product was taken up in dichloromethane and extracted in 10 % NaOH until the aqueous phase remained colorless. The organic phase was then acidified, dried, and extracted, and the solvent was removed as above to get product **9** to yield 6.24 g. Yield = 67 %, m.p. 126–130 °C [20].

Synthesis of 8-hydroxy-2,3,6,7-tetrahydro-1 H,5 H-pyrido[3,2,1-ij]quinoline-9-carbaldehyde 10

Phosphorous oxychloride (2.7 mL, 4.4 g, 29 mmol) was added dropwise in flask containing 10 mL DMF for a period of 15 min at 4 °C. A solution of 8-hydroxyjulolidine **7** (5.15 g, 26.9 mmol) in DMF (5 mL) was then added dropwise to the complex over period of 10 min. When the addition was complete, the reaction was stirred at room temperature for 30 min, and then heated at 100 °C for 30 min. After cooling to room temperature, 30 mL of water was added to the stirred dark solution. The aqueous mixture was stirred for 1.5 h resulting in the formation of a blue-green precipitate. The precipitate was isolated by filtration, washed with water and dried. The crude product was purified by column chromatography on silica gel (Toluene/EtOAc, 2:1) Yield = 94 %, m.p. 73–74 °C [20].

Synthesis of Iminocoumarin 11

2-cyano methyl benzimidazole **1** (0.55 g, 2.8 mmol), piperidine (0.1 mL, 1.4 mmol) was added in 50 mL of dry methanol, and the solution was stirred at room temperature for 30 min. Then 8-hydroxy-2,3,6,7-tetrahydro-1 *H*,5 *H*-pyrido[3,2,1-*ij*]-quinoline-9-carbaldehyde **10** (0.49 g, 2.8 mmol) was added. The mixture was stirred for 5 h at room temperature, and the precipitate was collected by filtration. The compound was washed with dry methanol to remove the impurities or unreacted starting material, and dried under high vacuum to obtain a yellow solid 3-benzimidazole iminocoumarin **11.** Yield = 81 % [51].

Synthesis of Coumarin 12

A mixture of the iminocoumarin **11** (0.332 g 3 mmol) and the aromatic aldehyde **10** (3 mmol), piperidine (0.01 ml) in *n*-butanol (15 ml) was heated to reflux for 3 h, cooled, and left overnight. The precipitated solid was filtered off, washed with ethanol, and dried. Obtained yellow colored solid **12** was purified by column chromatography, m.p. 235 °C.

12: Yield = 71 %, Orange red color solid, **^{1}H NMR** ($CDCl_3$, 500 MHz) δ ppm :1.60 (t, 4H), 1.99 (t, 4H), 2.63 (t, 4H), 2.78(t, 4H), 2.85 (broad, 4H), 3.69 (s, 6H), 6.61–6.72 (broad, 4H, −Ar), 7.02 (s, 1H), 7.69–7.75 (broad, 4H, −Ar), 8.83 (s, 1H), 9.76 (s, 1H), **^{13}C NMR** ($CDCl_3$, 125 MHz) δ ppm: 21.2, 22.7, 29.7, 46.6, 49.8, 50.2, 64.8, 106.0, 106.6, 108.7, 111.2, 111.1, 119.7, 122.5, 126.0, 126.4, 128.8, 129.3, 132.2, 142.9, 147.5, 148.5, 151.3, 151.8, 162.3, 171.5, 171.8, FT-IR(cm^{-1}): 2929 (−C-H), 2851 (aliphatic, −CH), 1730 (carbonyl), 1687 (−C=N), 1592, 1560 (−C=C-, aromatic), 1522 (−C=C-), **Mass**: m/z 632.3 $[M + 1]^+$.

Conclusion

In summary, synthesised iminocoumarin have interesting fluorescence properties. A large stokes shift and high quantum yield, good solubility in a wide range of solvents make these dyes more demanding and attractive for applications as fluorescent marker. The iminocoumarin **12** shows red shifted absorption and emission as compared to compounds **5a** and **5b**. In dye **12** rigid fixing of the electron donor nitrogen by two saturated six-membered heterocycles leads to red shift in absorption and emission. All the dyes are sensitive towards the solvent polarity, they show good quantum yield in polar and moderately polar solvents. The photophysical properties of the synthesized dyes were supported by DFT and it was observed that computational results are good agreement with the theoretical observations.

Acknowledgments Santosh B. Chemate is thankful for JRF and SRF fellowship from the Principal Scientific Adviser (PSA), Government of India for project stand-off detection of explosive based on immunoassay technique.

References

1. Li H, Cai L, Li J, et al. (2011) Novel coumarin fluorescent dyes: synthesis, structural characterization and recognition behavior towards Cu(II) and Ni(II). Dyes Pigments 91:309–316. doi:10.1016/j.dyepig.2011.05.011
2. Bochkov AY, Akchurin IO, Dyachenko OA, Traven VF (2013) NIR-fluorescent coumarin-fused BODIPY dyes with large stokes shifts. Chem Commun (Camb) 49:11653–11655. doi:10.1039/c3cc46498a
3. Signore G, Nifosì R, Albertazzi L, Bizzarri R (2009) A novel coumarin fluorescent sensor to probe polarity around biomolecules. J Biomed Nanotechnol 5:722–729. doi:10.1166/jbn.2009.1089
4. Valeur B (2001) Molecular fluorescence Principles and Applications.
5. Kumar S, Singh P, Srivastava R, et al. (2014) Engineering fused coumarin dyes: a molecular level understanding of aggregation quenching and tuning electroluminescence via alkyl chain substitution. J Mater Chem C. doi:10.1039/C4TC00807C
6. Liu Y, Zhang S, Lv X, et al. (2014) Constructing a fluorescent probe for specific detection of cysteine over homocysteine and glutathione based on a novel cysteine-binding group but-3-yn-2-one. Analyst 139:4081–4087. doi:10.1039/c4an00639a
7. Widmer S, Dorrestijn M, Camerlo A, et al. (2014) Coumarin meets fluorescein: a förster resonance energy transfer enhanced optical ammonia gas sensor. Analyst 139:4335–4342. doi:10.1039/c4an00061g
8. Micali G, Curro P, Calabro G (1984) High-performance liquid chromatographic separation and determination. Analyst 109:155–158
9. Komatsu K, Urano Y, Kojima H, Nagano T (2007) Development of an iminocoumarin-based zinc sensor suitable for ratiometric fluorescence imaging of neuronal zinc. J Am Chem Soc 129:13447–13454. doi:10.1021/ja072432g
10. Sun Q, Qian J, Tian H, et al. (2014) Rational design of biotinylated probes: fluorescent turn-on detection of (strept)avidin and bioimaging in cancer cells. Chem Commun (Camb) 50:8518–8521. doi:10.1039/c4cc03315a
11. Kim J, Park J, Lee H, Kim Y (2014) A boronate-based fluorescent probe for the selective detection of cellular peroxynitrite. chem comm. doi: 10.1039/c4cc02943g
12. Jones G, Rahman MA (1994) Fluorescence properties of coumarin laser dyes in aqueous polymer media. Chromophore isolation in poly(methacry1ic acid) hypercoils. J Phys Chem 8:13028–13037
13. Wlodarczyk P, Komarneni S, Roy R, White WB (1996) Enhanced fluorescence of coumarin laser dye in the restricted geometry of a porous nanocomposite. J Mater Chem 6:1967. doi:10.1039/jm9960601967
14. Hong SW, Ahn CH, Huh J, Jo WH (2006) Synthesis of a PEGylated polymeric pH sensor and its pH sensitivity by fluorescence resonance energy transfer. Macromolecules 39:7694–7700. doi:10.1021/ma061175h
15. Hara K, Sato T, Katoh R, et al. (2003) Molecular design of coumarin dyes for efficient dye-sensitized solar cells. J Phys Chem B 107:597–606. doi:10.1021/jp026963x
16. Sánchez-de-Armas R, San Miguel MÁ, Oviedo J, Sanz JF (2012) Coumarin derivatives for dye sensitized solar cells: a TD-DFT study. Phys Chem Chem Phys 14:225–233. doi:10.1039/c1cp22058f
17. Southgate PD (1971) Nonlinear optical susceptibility of a crystalline coumarin dye. J Appl Phys 42:4480. doi:10.1063/1.1659797
18. Ranjith C, Vijayan KK, Praveen VK, Kumar NSS (2010) Photophysical investigation of 3-substituted 4-alkyl and/or 7-acetoxy coumarin derivatives–a study of the effect of substituents on fluorescence. Spectrochim Acta A Mol Biomol Spectrosc 75:1610–1616. doi:10.1016/j.saa.2010.02.027
19. Khemakhem K, Ammar H, Abid S, et al. (2013) Spectroscopic study of 3-aryl-7-methoxy-coumarin, iminocoumarin and bis-iminocoumarin derivatives in solution. Dyes Pigments 99:594–598. doi:10.1016/j.dyepig.2013.06.003
20. Van Gompel J, Schuster GB (1987) Chemiluminescence of organic peroxides: intramolecular electron-exchange luminescence from a secondary perester. J Org Chem 52:1465–1468. doi:10.1021/jo00384a015
21. Lemieux G a, De Graffenried CL, Bertozzi CR (2003) A fluorogenic dye activated by the staudinger ligation. J Am Chem Soc 125:4708–4709. doi:10.1021/ja029013y
22. Anufrik SS, Tarkovsky VV, SG G, Asimov MM (2012) New laser dyes based on 3-imidazopyridylcoumarin derivatives. J Appl Spectrosc 79:46–52
23. Gorobets NY, Abakumov VV (2002) 3-(benzimidazolyl-2)-2-iminocoumarins in reactions with aromatic aldehydes. Chem Heterocycl Compd 38:1518–1520. doi:10.1023/A:1022605930640
24. Maslov VV, Gorobets NY, Borisov AV, Nikitchenko VM (2003) New series of dyes for flashlamp-excited lasers. J Appl Spectrosc 70:794–799. doi:10.1023/B:JAPS.0000008880.76919.05
25. Huang S-T, Jian J-L, Peng H-Z, et al. (2010) The synthesis and optical characterization of novel iminocoumarin derivatives. Dyes Pigments 86:6–14. doi:10.1016/j.dyepig.2009.10.020
26. Ahamed BN, Ghosh P (2011) Selective colorimetric and fluorometric sensing of Cu(II) by iminocoumarin derivative in aqueous buffer. Dalton Trans 40:6411–6419. doi:10.1039/c1dt10177c
27. Kim T, Jeong MS, Chung SJ, Kim Y (2010) An iminocoumarin-based fluorescent probe for the selective detection of dual-specific protein tyrosine phosphatases. Chem - A Eur J 16:5297–5300. doi:10.1002/chem.201000154
28. Fan X, Sen LYZ, Zhang XY, Qu GR (2006) A n Efficient and Green Synthesis of 1, 4-Dihydropyridine Derivatives through Multi-Component Reaction in Ionic Liquid. Heteroat Chem 17:382–388. doi:10.1002/hc
29. Turki H, Abid S, Fery-Forgues S, El Gharbi R (2007) Optical properties of new fluorescent iminocoumarins: part 1. Dyes Pigments 73:311–316. doi:10.1016/j.dyepig.2006.01.001
30. Kand D, Sahebrao P, Datar A, Talukdar P (2014) Iminocoumarin based fl uorophores: Indispensable scaffolds for rapid, selective and sensitive detection of thiophenol. Dyes Pigments 106:25–31. doi:10.1016/j.dyepig.2014.02.001
31. Fakhfakh M, Turki H, Fery-Forgues S, El Gharbi R (2010) The synthesis and optical properties of novel fluorescent iminocoumarins and bis-iminocoumarins: investigations in the series of urea derivatives. Dyes Pigments 84:108–113. doi:10.1016/j.dyepig.2009.07.003
32. Chemate S, Sekar N (2015) Highly sensitive and selective chemosensors for Cu 2+ and Al 3+ based on photoinduced electron transfer (PET) mechanism. RSC Adv 5:27282–27289. doi:10.1039/C5RA00123D
33. Bokanov AI, Turchin KF, Sedov IAL, Granik VG (1999) Cyanoethylation of 2-cyanomethylbenzimidazole. Pharm Chem J 33:94–97
34. Detert H, Schmitt V (2006) Acidochromism of stilbenoid chromophores with ap-aminoaniline centre. J Phys Org Chem 19:603–607. doi:10.1002/poc.1091
35. Lippert E (1957) Spektroskopische bestimmung des dipolmomentes aromatischer verbindungen im ersten angeregten singulettzustand. Zeitschrift für Elektrochemie, Berichte der

Bunsengesellschaft für Phys Chemie 61:962–975. doi: 10.1002/bbpc.19570610819.
36. Valeur B, Berberan-Santos MN (2012) Molecular Fluorescence: Principles and Applications 569.
37. Bilot L, Kawski A (1962) Zur theorie des einflusses von lösungsmitteln auf die elektronenspektren der moleküle. Zeitschrift für Naturforsch A. doi: 10.1515/zna-1962-0713.
38. Carlotti B, Flamini R, Kikaš I, et al. (2012) Intramolecular charge transfer, solvatochromism and hyperpolarizability of compounds bearing ethenylene or ethynylene bridges. Chem Phys 407:9–19. doi:10.1016/j.chemphys.2012.08.006
39. Frisch MJ, Trucks GW, Schlegel HB, et al. (2009) Gaussian 09, Revision C.01. Gaussian 09, Revis. B.01, Gaussian, Inc., Wallingford CT.
40. Stephens PJ, Devlin FJ, Chabalowski CF, Frisch MJ (1994) Ab initio calculation of vibrational absorption and circular dichroism spectra using density functional force fields. J Phys Chem 98:11623–11627. doi:10.1021/j100096a001
41. Becke AD (1988) Density-functional exchange-energy approximation with correct asymptotic behavior. Phys Rev A 38:3098–3100
42. Becke AD (1993) A new mixing of hartree–fock and local density functional theories. J Chem Phys 98:1372–1377
43. Lee C, Yang W, Parr RG (1988) Development of the colle-salvetti correlation-energy formula into a functional of the electron density. Phys Rev B 37:785–789. doi:10.1103/PhysRevB.37.785
44. Saranya G, Kolandaivel P, Senthilkumar K (2011) Optical absorption and emission properties of fluoranthene, benzo[k]fluoranthene, and their derivatives. A DFT study. J Phys Chem A 115:14647–14656. doi:10.1021/jp208617s
45. Zhao Y, Truhlar D (2008) The M06 suite of density functionals for main group thermochemistry, thermochemical kinetics, noncovalent interactions, excited states, and transition elements: two new functionals and systematic testing of four M06-class functionals and 12 other function. Theor Chem Accounts 120:215–241. doi:10.1007/s00214-007-0310-x
46. Fakhfakh M, Turki H, Abid S, et al. (2007) Preparation and optical properties of new fluorescent iminocoumarins: study of N-acyl-derivatives. J Photochem Photobiol A Chem 185:13–18. doi:10.1016/j.jphotochem.2006.04.036
47. Ware WR, Rothman W (1976) Relative fluorescence quantum yields using an integrating sphere. The quantum yield of 9,10-diphenylanthracene in cyclohexane. Chem Phys Lett 39:449–453. doi:10.1016/0009-2614(76)80301-6
48. Williams ATR, Winfield SA, Miller JN (1983) Relative fluorescence quantum yields using a computer-controlled luminescence spectrometer. Analyst 108:1067. doi:10.1039/an9830801067
49. Dhami S, De M a J, Rumbles G, et al. (1995) Phthalocyanine fluorescence at high concentration: dimers or reabsorption effect? Photochem Photobiol 61:341–346. doi:10.1111/j.1751-1097.1995.tb08619.x
50. Dalapati S, Jana S, Guchhait N (2011) Colorimetric "naked-eye" highly selective detection of Cu(II) ion by a simple chemosensor: an experimental and theoretical modeling. Chem Lett 40:279–281. doi:10.1246/cl.2011.279
51. Frath D, Poirel A, Ulrich G, et al. (2013) Fluorescent boron(III) iminocoumarins (boricos). Chem Commun (Camb) 49:4908–4910. doi:10.1039/c3cc41555d